Pergamon

Phys. Chem. Earth (C), Vol. 26, No. 1-3, pp. 201–205, 2001

1464-1917/00/$ - see front matter

PII: S1464-1917(00)00108-2

FAST Observations of Inertial Alfvén Waves and Electron Acceleration in the Dayside Aurora

C. C. Chaston, W. J. Peria, C. W. Carlson, R. E. Ergun and J. P. McFadden

Space Sciences Laboratory, University of California, Berkeley

Received 14 January 2000; revised 5 May 2000; accepted 30 June 2000

Abstract. A prevailing feature of small scale ($k_\perp c/\omega_{pe} \sim \geq 1$) Alfven waves observed from the FAST spacecraft is an association of the impulsive wavefield with bursts of field-aligned electrons with energies of the order of $1/2 m_e V_A^2$. The accelerated distributions have broad energy spectra up to a few 100 eV and are predominantly directed downwards although upward accelerated beams are sometimes observed. Observations show that the direction of acceleration is correlated with the direction of the wave Poynting flux and anti-correlated with the direction of the field-aligned current carried by the wave. The accelerated portion of the distribution in some cases carries all the field-aligned current since the thermal population is depleted. These observations are compared with the predictions of a 1-D MHD model (with an inertial correction) (Chaston et al., 2000) and a fluid-kinetic model (Clark and Seyler, 1999) for waveforms where $k_\perp c/\omega_{pe} \sim 1$ and $k_\perp c/\omega_{pe} >> 1$ respectively.

1 Introduction

Inertial Alfven waves with $k_\perp c/\omega_{pe} \sim 1$ are observed by the FAST satellite when in the auroral oval from perigee at 350 km up to apogee at 4180 km. The observed properties of these waves confirm the observations made by Freja (Louarn et al., 1994; Wahlund et al., 1994; Stasiewicz et al., 1998; Volwerk et al., 1996). The waves are observed most commonly in and around the cusp and are often imbedded in regions of magnetosheath ion precipitation. Nightside observations are however not unusual. Perhaps one of the most outstanding features of these waves in the aurora is their association with suprathermal fluxes of downgoing field-aligned electrons. These accelerated electrons have energies from 10 eV up to 1 keV and sometimes higher on the nightside and may provide precipitating energy fluxes in excess of 10 ergs/cm^{2}s. Examining high resolution data shows that these fluxes consist of a series of bursts well correlated with the impulsive Alfven wave field.

In this brief presentation we present fields and particle data collected over an interval of Alfvenic activity typically observed in the cusp or boundary plasma sheet and show high resolution observations of the particle distributions observed within the Alfven wave. For widths less than $2\pi c/\omega_{pe}$ the electric field waveforms become steepened, spike like and increasingly electrostatic and so the comparison to modelling discussion is separated into observations where $k_\perp c/\omega_{pe} \sim 1$ and those where $k_\perp c/\omega_{pe} >> 1$. For the sake of brevity, a case study for each width is examined while results from statistical studies performed by the authors and published elsewhere are referenced. For an overall summary of the plasma environment in which these waves are observed and statistical results relating to observed wave properties the interested reader is referred to Chaston et al. (1999), Chaston et al. (2000), and Stasiewicz et al. (2000).

2 Electron acceleration

Figure 1 presents an interval of spiky electric and magnetic field data recorded by FAST while traversing the dayside auroral oval at an altitude of 1600 km. Part a) of this figure shows that at this time there was significant magnetosheath ion and electron precipitation with latitudinal energy dispersion indicative of a cusp crossing (Heikkila and Winningham, 1971). The interval between the crosshairs is expanded in part b) and contains sharp fluctuations in E and B with amplitudes of a few hundred mV/m and 40 nT that are the subject of this study. The slope of the magnetometer trace in a) shows that during the majority of the selected interval there is no distinct large scale field-aligned current system until the appearance of the region 1 current system (downwards) at the high latitude edge of the crosshaired interval. These features suggests that the event occurred on open field lines on the morning side edge of the magnetospheric cusp.

Calculation of the E_{N-S}/B_{E-W} ratio over the interval shown in b) yields values of 1.0×10^7 m/s or slightly larger

Correspondence to: C. C. Chaston

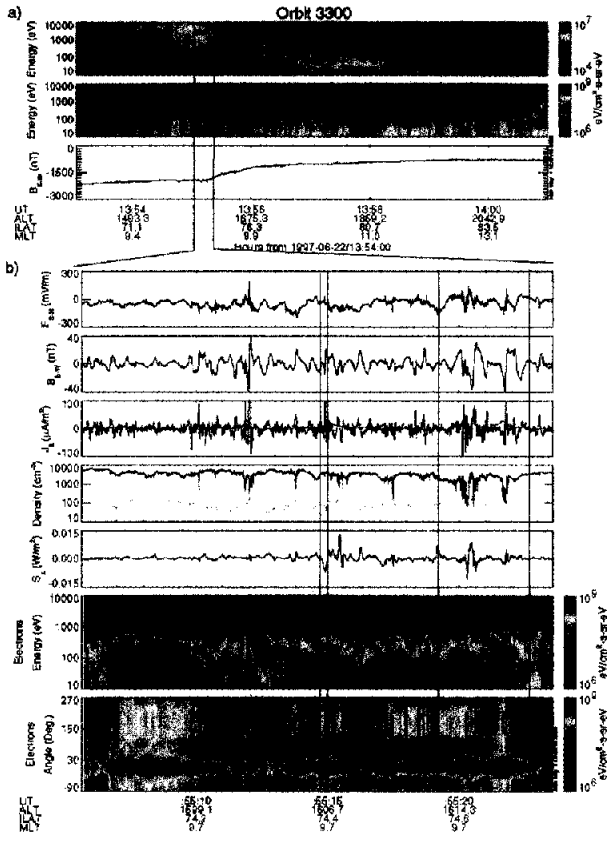

Fig. 1. Alfven waves in the cusp: a) Ion and electron energy spectra and the east-west magnetic field deflection from a cusp crossing. b) An expanded view of an interval from a) containing Alfvenic field fluctuations: the first panel shows the transverse to $\mathbf{B}_o$ wave electric field measured in the South-North direction; the second panel shows the transverse to $\mathbf{B}_o$ wave magnetic field measured in the East-West direction; the third panel shows the field-aligned current ($J_{||}$) determined from the magnetometer experiment where the purple line is the same determined from the electrostatic analyser experiment (esa) experiment; the fourth panel shows the density measured by the Langmuir probe where the blue trace is the same determined from the esa; the fifth panel is the field-aligned wave Poynting flux with positive values indicating downward propagating waves; the last two panels show the electron energy and pitch angle spectra with $0°$ being downward along $\mathbf{B}_o$. The vertical lines through b) show the intervals from which the two individual case studies considered are taken.

than the local Alfven speed for an oxygen dominated plasma at this altitude. This ratio is significantly larger than expected for static field-aligned currents when realistic dayside ionospheric Pedersen conductivity ratios are taken into account (Ishi et al., 1992). Each spike consists of one or two cycles with frequencies from 2-20 Hz in the spacecraft frame. Interferometric analysis using multi-point measurements suggest an average plasma frame frequency of $\sim$ 1 Hz (Stasiewicz et al., 2000) and an average perpendicular wavelength of 1 km or $k_\perp \lambda_e \sim 1.0 (\lambda_e = c/\omega_{pe})$ (Chaston et al., 1999). Using the assumption of a planar current sheet and that these field structures are time stationary (at least over the transit time of the spacecraft through the structure) the magnitude and direction of the field-aligned current carried by the wave can be estimated. The results from this approach (which are most likely an overestimate the current due to the contribution of $d\mathbf{B}_1/dt$ in the calculation of $\nabla \times \mathbf{B}_1$) are displayed in the third panel and show that the waves carry a very localised yet intense (by auroral standards) field-aligned current with magnitudes at times of over 100 μ A/m^2. Determining the current measured by the electrostatic analyser (esa) experiment onboard the spacecraft (purple trace third panel) show that for each spike a significant portion is carried by energetic (>4eV) electrons. Under such conditions it seems unlikely that the field-lines here approximate equipotentials as assumed in the usual analysis of field-aligned currents and E/B ratios as performed by Sugiura et al. (1984), but rather suggests the existence of parallel to $\mathbf{B}_o$ electric fields. Furthermore, the large currents measured by the esa suggest a depletion of the cold plasma density within the Alfven wavefield as indicated in the fourth panel. The black trace here is the density determined from the calibrated Langmuir probe (Chaston et al., 1999) and the blue shows the density measured by the esa experiment. Note how each depletion in total electron density measured by the Langmuir probe is anti-correlated with an enhancement in the energetic electron density and that at times the densities agree thereby suggesting a total absence of cold plasma within the cavity in such events.

With such intense fluxes of energetic electrons found within the wavefield it is relevant to calculate the total wave energy density to determine if the wave is capable of accounting for the observed electron acceleration. The fifth panel of figure 1b) shows the field-aligned wave Poynting flux and indicates that these waves have predominately downgoing group velocities (positive S_z) with magnitude 10 or more times larger than the integrated electron energy flux. (Note: for an inertial Alfven wave the phase and group velocities along $\mathbf{B}_o$ are aligned). From this observation it seems certainly possible that Alfven wave can account for the observed field-aligned fluxes. In fact, the spectral results displayed in the last two panels of Figure 1 show that each Alfvenic pulse observed is correlated with enhanced electron fluxes with energies up to 200 eV distributed as a narrow field-aligned beam travelling downwards (0°) towards the ionosphere. At times there is evidence for enhanced upwards (180°) fluxes. For a landau resonant process the parallel phase speed of the Alfven wave with an inertial correction may provide electron energies of up to 300 eV which is consistent with the observed electron energy spectra.

2.1 $k_\perp \lambda_e \sim 1$ and the Inertial Alfven Wave Model

Figure 2 a shows more closely the waveform of the Alfvenic fluctuations seen from FAST and is taken from the interval displayed in Figure 1. It is difficult to associate such fluctuations with a particular scale size or wavenumber however the low frequency spikes in E_{S-N} have a width such that $k_\perp \lambda e \sim 1.0$. The waveforms in E and B are similar although a clear phase difference is not apparent. The B field components are in anti-phase suggesting a planar geometry in $j_{||}$. Associated with these fluctuations, the fourth panel of

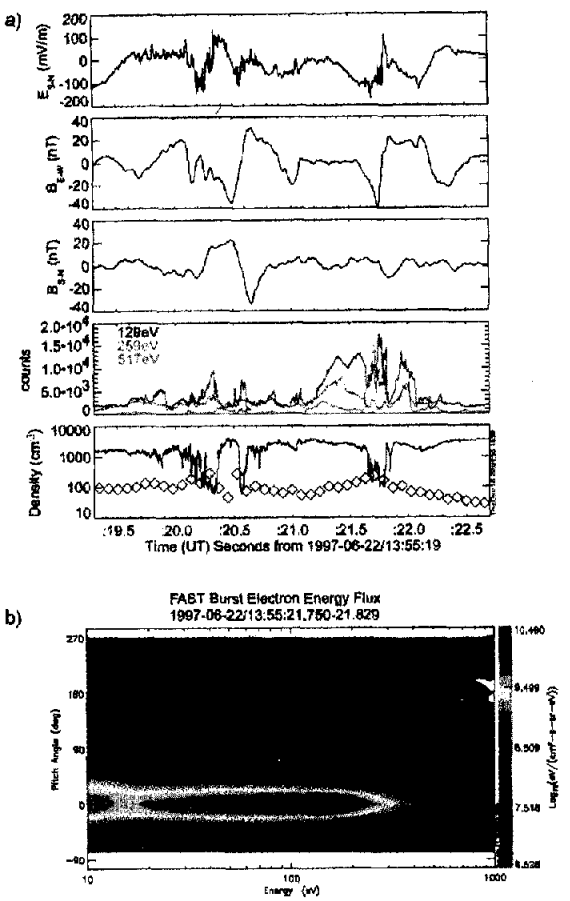

Fig. 2. a) Alfvenic turbulence with $k_\perp \lambda_e \sim 1$: the first panel shows the transverse to $\mathbf{B_o}$ wave electric field measured in the South-North direction; the second panel shows the transverse to $\mathbf{B_o}$ wave magnetic field measued in the East-West direction; the third panel shows the transverse to $\mathbf{B_o}$ wave magnetic field measured in the South-North direction; the fourth panel shows the counts recorded in field-aligned fixed energy channels up to 500eV; and the fifth panel shows the density measured by the Langmuir probe where the diamonds are the same determined from the esa measurements. b) Electron pitch angle distribution function.

figure 2a shows enhanced counts in the field-aligned low energy channels up to 500eV. The largest amplitude magnetic field oscillations are accompanied by deep ($\Delta n/n \sim 1$) density cavities (fifth panel) whose deepest extent match well the density determined from the electrostatic analyser experiment (diamonds) as mentioned above. For such examples the langmuir probe current matches the current due to energetic electrons incident on the probe (sphere) so it seems that in these cases the density probe measurements do provide a reliable indication of the total electron density and that the density cavities are real.

The pitch angle distribution function shown in Figure 2b was measured within the density cavity observed at 13:55:21.75 UT shown in 2a and is typical of distributions measured coincident with Alfvenic wave activity with $k_\perp \lambda_e \sim 1.0$. Chaston et al. (2000), using the 1-D inertial MHD formalism developed by Thompson and Lysak (1996), has shown how ambient ionospheric electrons can be accelerated by an inertial Alfven wave in a magnetic field-aligned density gradient to form the broad (in energy) field-aligned component observed. For a detailed description of this model the interested reader is referred to Chaston et al. (2000). Briefly however, in this model, the wavefield of a Alfven wave propagating into the density and magnetic field gradients present in the topside ionosphere is followed by solving a generalised Ohm's law including electron inertia which allows a parallel to B_0 wavefield to exist. Qualitatively, the broad suprathermal component (STEB) results from Landau resonant acceleration in this parallel wave which for altitudes below $\sim$ 2000 km has decreasing amplitude and phase speed with decreasing altitude. Consequently ionospheric electrons which interact with the wave at lower altitudes gain less energy than those at higher altitudes and so the superposition of electrons accelerated at different altitudes results in a broad (in energy) field-aligned component below 100 eV. Since the temperature of the source ionspheric population is of the order of an eV the electrons of ionospheric origin form a fine (in pitch-angle) field-aligned beam. In addition, magnetosheath electrons also interact with the Alfven wave. Temperatures of this component are of the order of $\sim$ 100eV and these form the broader in pitch angle fluxes observed at a few hundred eV. Since these electrons initially interact with the wave at higher altitudes they gain more energy than the ionospheric component and their mirrored portion may lead to the formation of electron conics as discussed by other authors (Thompson and Lysak, 1996).

2.2 $k_\perp \lambda_e >> 1$ and the Self Induced Trapping Model

Seyler and Wahlund (1996) and Seyler et al. (1998) have shown how an inertial Alfven wave may advectively steepen and evolve into higher wavenumber forms described as 'slow ion acoustic' or electron acoustic waves. These essentially electrostatic waves have wavelengths less than the electron skin depth and may accelerate electrons to energies of up to mV_A^2. The mechanism for electron acceleration is described as self-induced trapping (Clark and Seyler, 1999) and proceeds via a 'kick' onto trapped particle orbits that the ambient electron population receives as steepened wavefield or spike passes through the plasma.

Waveforms consistent with the steepening process are sometimes observed from FAST particularly at lower altitudes. Figure 3 shows a waveform captured during the interval presented in Figure 1. The electric field component (E_{S-N}) here is taken from a sphere pair with separation of 5m to eliminate finite wavelength effects which occur for these shorter scale structures. Consequently the amplitude shown is larger than it appears in Figure 1b). The waveform consists of a single cycle pulse or spike with width much narrower than the corresponding B field fluctuation (this has been verified by examining the waveform from the search coil magnetometer). Using the ambient density at this time ($\sim$3000

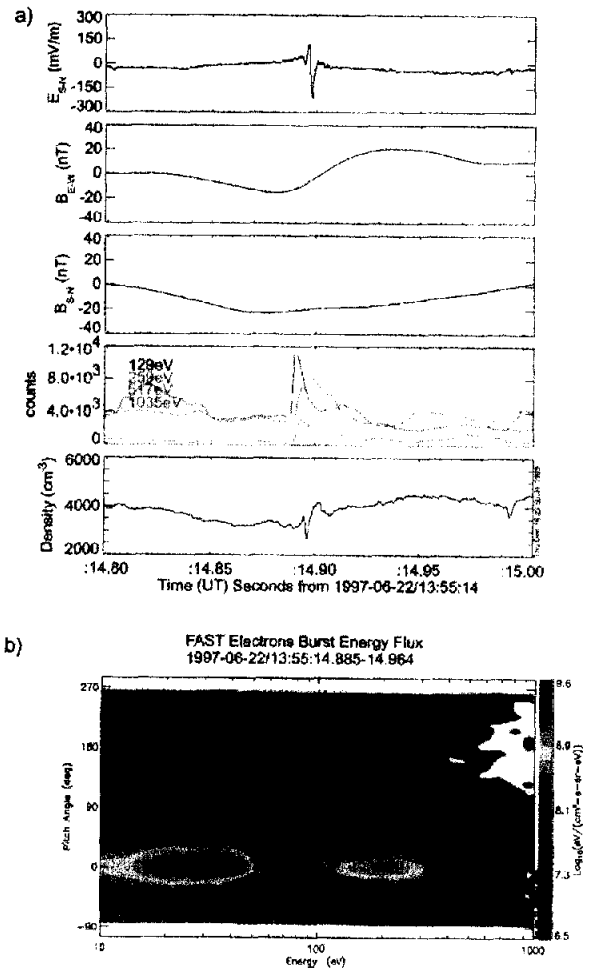

Fig. 3. a) Alfvenic pulse or spike with $k_\perp \lambda_e >> 1$: the first panel shows the transverse to $\mathbf{B}_o$ wave electric field measured in the South-North direction; the second panel shows the transverse to $\mathbf{B}_o$ wave magnetic field measured in the East-West direction; the third panel shows the transverse to $\mathbf{B}_o$ wave magnetic field measured in the South-North direction; the fourth panel shows the counts recorded in field-aligned fixed energy channels up to 1 keV; and the fifth panel shows the density measured by the Langmuir probe. b) Electron pitch angle distribution function.

cm^{-3}) and interpreting the structure as a predominately spatial feature (Chaston et al., 1999) yields $k_\perp \lambda_e \sim 10.0$. Coincident with the spike and persisting for ~20ms after the spike is an abrupt enhancement in electron counts in the downgoing field-aligned angle bins from the lowest energies recorded to greater than 1 keV with no clear dispersive character present.

Interferometric determination shows that in the satellite frame the waveform travels from the right to the left in the figure shown or antiparallel to the spacecraft trajectory in the plane perpendicular to $\mathbf{B}_o$ at a speed of ~0.4 km/s. However since this is of the order of the expected $\mathbf{E} \times \mathbf{B}_o$ drift velocity at this altitude it is not clear if in the plasma frame the spacecraft overtakes the wave from behind or alternatively has a head-on collision with the wave. The later interpretation provides results consistent with the theory. In this case the wave propagates to the left and electrons trapped in the potential well of the wave follow behind the wavefront with speeds up to twice the parallel wave phase speed or ~600eV. If conversely, the spacecraft were to overtake the wave from behind then we would expect to see enhanced energetic fluxes shortly before passing through the wavefront and then a sudden decrease once when the spacecraft has passed the spike by (i.e the exact reverse of what is observed). Another similarity between this theory and the observations is that the waveform when inverted (due to its reverse direction of propagation in the figure) is very similar to the predicted waveform shown in figure 1d(iii) of Clark and Seyler (1999). Finally, the pitch angle distribution shown in figure 3b) does not greatly differ in form to that measured in coincidence with the smaller $k_\perp$ structures discussed in section 2.1. If the trapping process described in this model were to operate over a range of altitudes then a broad (in energy) field-aligned beam could be expected to form for the same reasons discussed for the $k_\perp \lambda_e \sim 1$ case albeit at somewhat smaller energies due to the inverse scaling of phase speed with $k_\perp$.

Two essential features of the model are however difficult to confirm in the data. Firstly, the steepening process as described in the model should result in a density enhancement colocated with a negative field spike. Density measurements from the Langmuir probe instrument onboard FAST typically indicate density depletions (Chaston et al., 2000) rather than humps in association with the wavefield and the position in which the density measurement is taken for these very narrow features (~50m) is significantly displaced from the electric field measurement. As a consequence, the distinctive ion-Boltzmann character ($\delta n_i \approx -e\delta\phi/Ti$) of the expected wave is difficult to verify. For the example shown in figure 3a the Langmuir probe current (fifth panel) is bipolar indicating a sharp depletion followed by a broader enhancement of roughly equal magnitude. While the broader cavities, as discussed above, seem reliable measurements (based on independent confirmation form the esa experiment), for the very fine scale structures, where rapidly varying electric fields exist, it is of course possible that the Langmuir probe density measurement is unreliable and so cannot be used as a test of the theories validity. The second feature which is difficult to confirm is the requirement that $T_i/T_e >> 1$ for the 'slow ion acoustic' wave to propagate without significant electron Landau damping. FAST observations of low energy ions in regions where these waves occur often indicate enhanced energies which may allow the slow ion acoustic wave to propagate, however this is not always the case. In fact in those cases where a warmer ion population is observed it appears that these ions result from heating within the wavefield itself rather than as a condition which existed apriori.

3 Conclusions

Since the initial work of Hasegawa (1976) electron acceleration by Alfven waves has been a topic of continuing interest in auroral physics and space plasmas generally. However, there has been little direct comparison between the observed

accelerated electrons, thought to be associated with these waves, and the predictions of theory. In this report we have attempted to directly compare the observed fields and particle data with the predictions of a 1-D 'MHD' test particle model (Thompson and Lysak, 1996; Chaston et al., 2000) which includes the macroscopic properties of the auroral ionosphere, with those of a self-consistent fluid kinetic model (Clark and Seyler, 1999) providing details of the waveform evolution and electron acceleration on smaller perpendicular scales.

Since the 'MHD' model includes altitude dependent wave phase speeds and magnetic fields the details of the entire pitch angle distribution can be reproduced and compared directly with the observed distribution. Good qualitative agreement between observations and theory is found when contributions from different electron source regions and realistic density profiles are included. However, this agreement can only ever be qualitative and will not address the inherently non-linear aspects of the wave-particle interaction including density fluctuations and steepened waveforms. The fluid-kinetic model includes such effects to yield waveforms similar to those observed yet predicts density humps when cavities are observed and is reliant upon Ti/Te $>>1$, a situation which does not prevail in the auroral ionosphere.

Acknowledgements. This research was supported by NASA grant NAG5-3596.

References

Chaston, C. C., Carlson, C. W., Peria, W. J., Ergun, R. E., and McFadden, J. P., FAST observations of inertial Alfven waves in the dayside aurora, *Geophys. Res. Lett.*, *26*, 647-650, 1999.

Chaston, C. C., Carlson, C. W., Ergun, R. E., and McFadden, J. P, Alfven waves, density cavities and electron accleration observed from the FAST spacecraft, *Physica Scripta*, *T84*, 64–68, 2000.

Clark, A. E., and Seyler, C. E., Electron beam formation by small-scale oblique inertial Alfven waves, *J. Geophys. Res.*, *104*, 17233–17249, 1999.

Hasegawa, A., Particle acceleration by MHD surface wave and formation of aurora, *J. Geophys. Res.*, *81*, 5083–5090, 1976.

Heikkila, W. J., and Winningham, J. D., Penetration magnetosheath plasma to low altitudes through the dayside magnetospheric cusps, *J. Geophys. Res.*, *76*, 883–891, 1971.

Ishi, M. Sugiura, M., Iyemori, T., and Slavin, J. A., Correlation between magnetic and electric field perturbations in field-aligned current regions deduced from DE-2 observations, *J. Geophys. Res. 97*, 13877-13887, 1992.

Louarn, P., Wahlund, J. E., Chust, T., de Feraudy, H., Roux, A., Holback, B., Dovner, P. O., Eriksson, A. I., and Holmgren, G., Observation of kinetic Alfven waves by the Freja spacecraft, *Geophys. Res. Lett.*, *21*, 1847–1850, 1994.

Seyler, C. E., Wahlund, J.-E., Theory of nearly perpendicular electrostatic plasma waves and comparison to Freja satellite observations, *J. Geophys. Res.*, *101*, 21795–21813, 1996.

Seyler, C. E., Clark, A. E., Bonnell, J., and Wahlund, J.-E., Electrostatic broadband ELF wave emission by Alfven wave breaking, *J. Geophys. Res.*, *103*, 7027–7041, 1998.

Stasiewicz, K., Holmgren, G., and Zanetti, L., Density depletions and current singularities observed by Freja, *J. Geophys. Res.*, *103*, 4251–4260, 1998.

Stasiewicz, K., Bellan, P., Chaston, C., Kletzing, C., Lysak, R., Maggs, J., Pokhotelov, O., Seyler, C., Shukla, P., Stenflo, L., Streltsov, A., and Wahlund, J. E., Small-scale Alfvenic structure in the aurora, *Space Sci. Rev.*, in press, 2000.

Sugiura, M., Iyemori, T., Hoffman, R. A., Maynard, N. C., Burch, J. L., and Winningham, J. D., Relationships between field-aligned currents, electric fields, and particle precipitation as observed by Dynamics Explorer-2, *Geophys. Monog. 28*, T. A. Potemra, ed., American Geophysical Union, pp-96-103, 1984.

Thompson, B. J., and Lysak, R. L., Electron acceleration by inertial Alfven waves, *J. Geophys. Res.*, *101*, 5359–5369, 1996.

Volwerk, C., Louarn, P., Chust, T., Roux, A., de Feraudy, H., and Holback, B., Solitary kinetic Alfven waves: a study of the Poynting flux, *J. Geophys. Res.*, *101*, 13335–13343, 1996.

Wahlund, J.-E., Louarn, P., Chust, T., de Feraudy, H., Roux, A., Holback, B., Dovner, P.-O., and Holmgren, G., On ion acoustic turbulence and the nonlinear evolution of kinetic Alfven waves in aurora, *Geophys. Res. Lett.*, *21*, 1831–1834, 1994.